Journal of Applied Polymer Science

Glutaraldehyde-crosslinked Chitosan/Hydroxyapatite Bone Repair Scaffold and its Application as Drug Carrier for Icariin

Yan Li,[1,2] Taotao Liu,[2] Jun Zheng,[3] Xiaoyan Xu[1,2]

[1]Key Laboratory of Advanced Civil Engineering Materials of Ministry of Education, Shanghai 201804, China

[2]School of Materials Science and Engineering, Tongji University, Shanghai 201804, China

[3]Shanghai University of Traditional Chinese Medicine, Yueyang Hospital of Integrated Chinese and Western Medicine, Shanghai 200437, China

Correspondence to: X. Xu (E-mail: kadxxy@tongji.edu.cn)

ABSTRACT: Chitosan/hydroxyapatite (CS/HA) bone repair scaffolds crosslinked by glutaraldehyde (GA) were prepared. Characterization of morphology, structure, mechanical property, and porosity of scaffolds were evaluated. The influences of CS viscosity, HA content, and crosslinking degree on properties of scaffolds were discussed. SEM images showed that CS/HA scaffolds were porous with short rod-like HA particles dispersing evenly in CS substrate. When $[\eta]_{CS} = 5.75 \times 10^{-4}$, HA content = 65%, and crosslinking degree = 10%, the resulting CS/HA scaffolds had a flexural strength of 20 MPa and porosity of 60%, which could meet the requirements of bone repair materials. The scaffolds were used as drug carriers for icariin, and the impacts of loading time and crosslinking degree of scaffolds on drug-loading dose were discussed. The suitable loading time was 24 h and it would be better to keep crosslinking degree no more than 10%. The drug release behavior demonstrated that the icariin-loading CS/HA scaffolds could achieve basic drug sustained release effect. © 2013 Wiley Periodicals, Inc. J. Appl. Polym. Sci. 000: 000–000, 2013

KEYWORDS: biomaterials; composites; crosslinking; porous materials; drug delivery systems

Received 28 September 2012; accepted 12 March 2013; Published online

DOI: 10.1002/app.39339

INTRODUCTION

Nowadays, the appearance and development of bone tissue engineering provide a new approach for the repair of bone defect caused by trauma, infection, tumor, and dysplasia. The ideal bone repair materials should have such properties: can imitate the morphology, structure, and function of bone;[1] have proper mechanical strength to meet the mechanical demand of the implanted parts;[2] have good biocompatibility;[3] have porous structure, with suitable aperture and porosity;[4] can act as a drug carrier.

Bone repair scaffolds are usually composed of inorganic and organic phases, which imitate the composition of bone tissue. There are several biocompatible inorganic materials such as calcium carbonate,[5] tricalcium phosphate (TCP),[6] hydroxyapatite, aluminum oxide,[7] carbon fiber,[8] etc. are frequently used to substitute for the inorganic component of bone. Many natural and synthetic polymers such as collagen,[9] gelatin,[10] chitosan, polyester,[11] polycaprolactone,[12] and so on, have been explored as the organic phase of bone repair scaffold. Among them hydroxyapatite and chitosan are two potential materials in common use.

Hydroxyapatite (HA) has the same chemical composition and crystal structure with the inorganic constituent of natural bone.[13] It is a biological activity material which has good biocompatibility and bone conduction.[14] Chitosan (CS) is a natural degradable polymer which possesses excellent biocompatibility and medicine activity.[15] Heinemann's research[16] shows that CS can enhance the differentiation capacity of bone precursor cells and promote the formation of bone. The composites combining CS and HA together have proper mechanical property and biocompatibility. Mukherjee et al.[17] prepared a starchiness CS/HA composite and applied it on the repair of rabbit skull defect. The mechanical test showed that the repaired tissue had similar impact strength with the normal tissue. Zan et al.[18] fabricated a CS/HA scaffold with a special shell structure through basification. The scaffold contained good compress strength of 6.85MPa, which was close to the strength of the cancellous bone.

Recently, several researchers combined bone repair materials with drugs or osteogenic active factors together to promote the repair and regeneration of bone tissue. Chen et al.[19] prepared a gentamicin-loaded chitosan bar and inserted it into the proximal portion of tibia in a rabbit. Result indicated that the gentamicin-loaded chitosan bar was a good biodegradable drug delivery system with sustained antibiotic effect *in vivo* and it

might be a clinical useful and simple method for the treatment of bone infection without a second operation for removal of the carrier. Epimedium sagittatum is a traditional Chinese medical herb and widely used in the therapies of fractures, bone and joint diseases for hundreds of years.[20] Icariin ($C_{33}H_{40}O_{15}$, molecular weight: 676.67), a typical flavonol glycoside, is considered to be the major pharmacological component of epimedium sagittatum.[21] Recent evidences indicated icariin can accelerate the osteogenesis from mesenchymal stem cells and suppress the activities of osteoclasts *in vitro*.[22] Thereby, icariin is a potential osteogenic inductive agent which can promote bone formation and inhibit bone resorption. Wu et al.[23] generated a new bone repair scaffold by mixing icariin into the CS/HA system. The result indicated that icariin-CS/HA had favorable cell compatibility and promoted osteogenic differentiation of hBMSCs; it could fill bone defect sites and stimulate the formation of newborn bone tissues at early stage.

There were many researchers prepared CS/HA composites through solution blending method in recent years.[24] However, few investigations had focused on the influential factor in the preparation process. In this article, we made a further study of this complex process, including the influences of CS viscosity and HA content. Simultaneously, to improve the mechanical property and stability of CS/HA scaffolds, glutaraldehyde (GA) was added to crosslink with CS, and the effect of crosslinking degree was discussed. In addition, the CS/HA scaffolds were used as drug carriers and icariin was loaded on the scaffolds. The impacts of loading time and crosslinking degree of scaffolds on drug-loading dose were discussed, and the drug release behavior of the icariin-loading CS/HA scaffolds was studied preliminarily.

EXPERIMENTAL

Materials

Chitosan (degree of deacetylation >90.0%) was purchased from Weifang Haizhiyuan Bio-products, China. Hydroxyapatite (biomedical grade, purity $\geq$ 96%) was purchased from Nanjing Emperor Nano-material, China. Icariin (Chemical reference substance, 110737-200415) was purchased from The National Institute for the Control of Pharmaceutical and Biological Products, China. Acetic acid (AR, content = 36%), glutaraldehyde (AR, content = 50%), NaOH (AR, purity $\geq$ 96%) and ethanol (AR, content $\geq$ 99%) were all purchased from Sinopharm Chemical Reagent, China. All reagents were used as received without further purification.

Preparation of CS/HA Scaffolds

A certain amount of CS was dissolved in 1% (v/v) acetic acid and concentration of CS solution was 2% (w/v). Then HA powders were added in the CS solution (HA content was 10, 33, 50, 65, and 75%, respectively). The CS/HA solution was stirred adequately and homogenized by ultrasonic. Afterwards, 0.1% (v/v) glutaraldehyde solution (GA content* was 0.02, 0.05, 0.1, 0.5, 1, and 2%) was dropped in the CS/HA solution in ice bath under 0°C. The resulting solution was put into molds which were placed at 25°C overnight for crosslinking. Then the samples were placed at −10°C for 6 h and freeze-dried at −50°C in a freeze dryer (FD-1, Beijing Boyikang Instrument, China). After they were fully dried, the CS/HA scaffolds were soaked in 1% (w/v) NaOH solution for 12 h, and then rinsed with deionized water for several times. Finally, the prepared scaffolds were frozen and freeze-dried again. The resulting CS/HA scaffolds were stored in a drying box at room temperature before subsequent use.

Preparation of Icariin-Loading-CS/HA Scaffolds

Icariin was dissolved in anhydrous ethanol and concentration of icariin solution was 1×10^{-5} mmol mL^{-1}, then CS/HA scaffolds were immersed into the icariin solution with continuous stirring. Several hours later, the scaffolds were taken out and freeze-dried. The icariin-loading-CS/HA scaffolds were stored at 4°C before subsequent use.

Characterization of the CS/HA Scaffolds

The morphological structure and apertures size distribution of the CS/HA scaffolds were examined by scanning electron microscope (SEM, Philips XL-30 ESEM, Philips, the Netherlands) at an accelerating voltage of 15 kV. The specimens were cut from the scaffolds and the cross-section was coated with gold for observation.

Fourier transform infrared spectra were obtained using Fourier transform infrared spectrometer (FTIR, EQUINOXSS, BRUKER, Germany). All spectra were taken in the range of 4000–400 cm^{-1} with a resolution of 2 cm^{-1}.

The crystallinity of CS/HA scaffolds was examined by X-ray spectrometer (XRD, Rigaku, Japan). All spectra were obtained with scanning scope of 10°–90°and scanning speed was 10° min^{-1}, using Cu Kα radiation with $r = 0.15418$ nm.

Dynamic mechanical thermal analysis (DMA, Q800, TA Instruments, USA) was used to analyze storage modulus of crosslinked CS specimens in dimensions of 15-mm long, 5-mm wide, and 0.2-mm thick. All curves were obtained in the tensile mode at a constant frequency of 1 Hz and a heating rate of 1°C min^{-1} from 25 to 80°C.

Mechanical Testing

The flexural strength of the CS/HA scaffolds was detected with universal testing machine (CMT5105, Shenzhen Sans Material Test Instrument, China). The size of samples was 80 × 10 × 1 mm^3. The speed of the testing machine crosshead was controlled at 10 mm min^{-1}.

Crosslinking Degree

The crosslinking degree of CS/HA scaffolds was measured by Soxhlet extractor. A certain amount (W_1) of CS/HA sample was wrapped by filter paper and placed into the extraction tube. The weight of CS in the sample was credited as W_0. Nearly 200 mL 1% (v/v) acetic acid was added into the extraction flask and heated to reflux for 24 h. Afterward, the sample which had been dried was weighed and the weight was credited as W_2. The crosslinking degree (CLD) was calculated according to formula (1):

$$CLD = \frac{W_0 - (W_1 - W_2)}{W_0} \times 100\% \quad (1)$$

Porosity

The porosity of CS/HA scaffolds was evaluated by liquid displacement method[25]: Added a certain volume (V_1) of ethanol

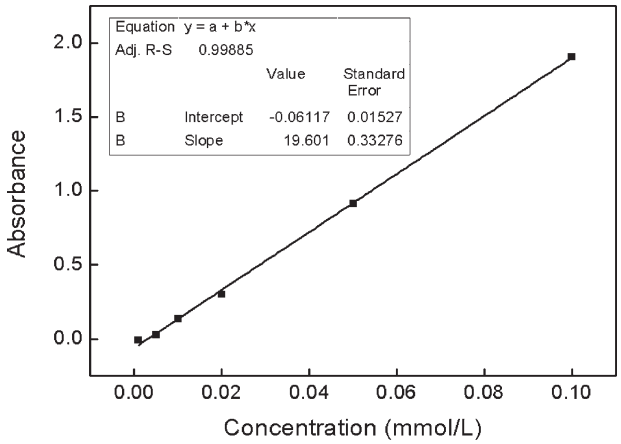

Figure 1. Icariin standard curve.

into a graduated cylinder. Then, the sample was immersed into ethanol until it was saturated by absorbing ethanol (no bubble escape from the CS/HA scaffold) and recorded the reading as V_2. After the sample was removed, the volume of solution remained was credited as V_3. The porosity (P) of the scaffold was calculated according to the formula (2).

$$P = \frac{V_1 - V_3}{V_2 - V_3} \times 100\% \quad (2)$$

Concentration of Icariin Solution

Ultraviolet absorption of icarrin can be detected by UV–vis spectrophotometer (UV759S, Shanghai Precision & Scientific Instrument, China) at 270 nm. The concentration of icariin solution was calculated by ultraviolet absorption and the standard curve of icariin. Icariin standard curve was obtained as follows: a precise amount of icariin was dissolved in anhydrous ethanol to prepare a series of standard solutions with concentrations of 0.001, 0.005, 0.01, 0.02, 0.05, and 0.1 mmol L^{-1}, respectively. Then ultraviolet absorption of these standard solutions was detected. Standard curve was drawn with concentration as X-coordinate and ultraviolet absorption as Y-coordinate. There was a good linear relationship between concentration of icariin standard solution and its ultraviolet absorption in the test range (Figure 1. The linear regression equation is:

$$Y = 19.601X - 0.06117 \quad (3)$$

The R value (R = 0.99885) of this equation is very close to 1, which indicates the validity of the standard curve and linear regression equation.

In Vitro Drug Release

Release behavior of icariin was analyzed by immersing icariin-CS/HA scaffold (icariin dose = 2.5×10^{-4}mmol cm^{-3}, CLD = 10%) in 10 mL phosphate buffer solution (PBS, 0.1 M, pH 7.4) and stirred continuously at 37°C. The amount of released icariin was determined by studying aliquot amounts of the sample solutions withdrawn at selected time intervals.

RESULTS AND DISCUSSION

Mechanical Property and Porosity of CS/HA Scaffold

Effect of HA Content. In the CS/HA scaffolds, HA particles are wrapped up in CS molecular chain and act as a strengthen-phase to help reinforce the composites. The flexural strength and porosity of the CS/HA scaffolds with different HA content of 10, 33, 50, 65, and 75% are provided in Figure 2. When HA content was 10%, the CS/HA scaffolds had a low flexural strength of 1.3 MPa. With the increase of HA content, mechanical strength of the CS/HA scaffolds showed a markedly improvement and the flexural strength reached a maximum value of 13.8 MPa when HA content was 65%. When HA content is low, the HA particles cannot form continuous distribution in the CS substrate. Therefore, the CS/HA scaffolds have loose structure and high porosity (75–85%), which lead to low flexural strength. The load applied on materials cannot be transferred between the inorganic phase and organic phase effectively.[26] As HA content increased, the flexural strength improved significantly. However, when HA content turned from 65 to 75%, the flexural strength of the CS/HA scaffold had a rapid decline. This may be due to the bad dispersion of HA particles when HA content is too high. This explanation is confirmed by SEM image of HA distribution (Figure 3. When the HA content was 65%, HA particles dispersed in the scaffold evenly and continuously. While the HA content was 75%, apparent agglomeration of HA could be observed which affect mechanical properties of the CS/HA scaffold. Han's research[4] shows that ideal bone repair materials demand porosity no <60% to act as a good drug carrier and be contributive for the growth of bone tissue. In our investigated range, the CS/HA scaffolds still had higher porosity (64.6%) even the HA content had arrived at 65%. Hence, 65% HA content is an optimum ratio for the preparation of CS/HA scaffold under which the scaffold have both high porosity and maximum flexural strength. This is also similar with the composition of natural bone (70% inorganic phase and 30% organic phase).

Effect of CS Viscosity. Because the molecular weight of CS is hard to be detected by GPC, the intrinsic viscosity [η] of CS

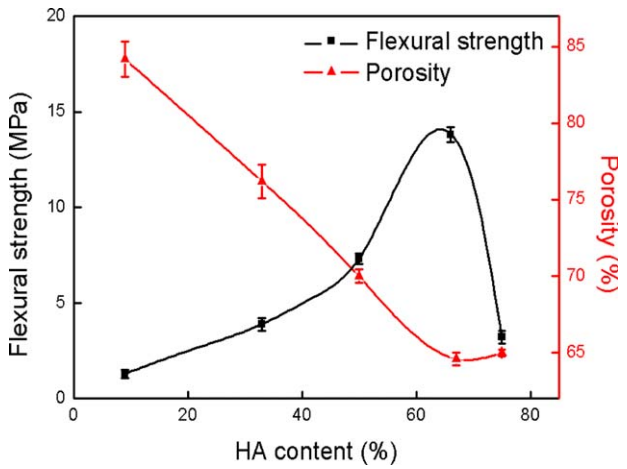

Figure 2. Effects of HA content on flexural strength and porosity of the CS/HA scaffolds. [Color figure can be viewed in the online issue, which is available at wileyonlinelibrary.com.]

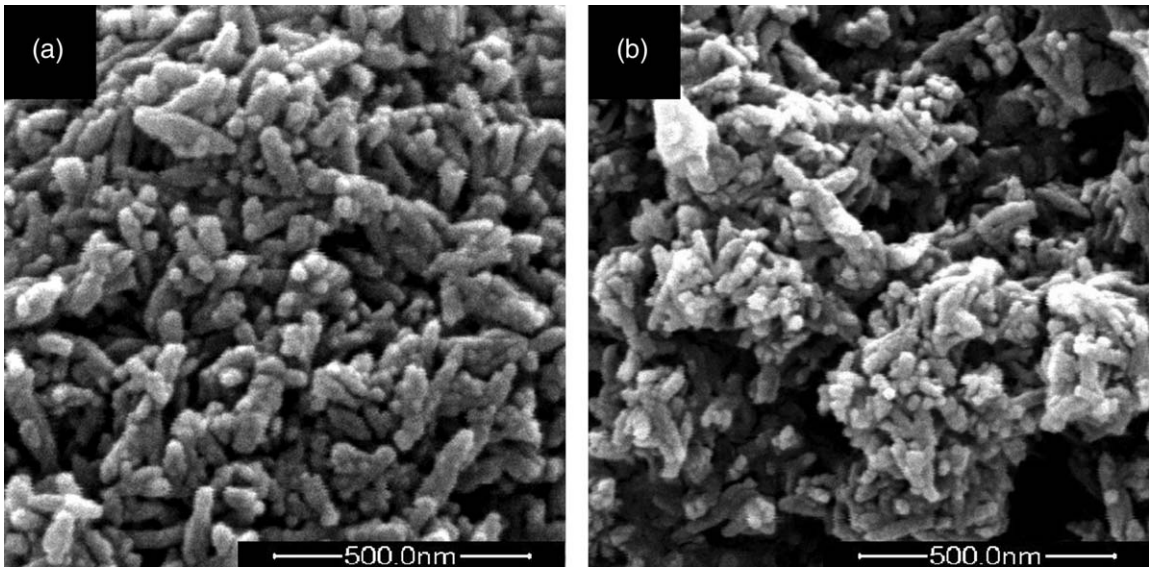

Figure 3. SEM images of HA particles dispersion in the CS/HA scaffolds: (a) HA content = 65%; (b) HA content = 75%.

was measured with Ubbelohde viscometer and its impact on properties of the CS/HA composites was studied (Figure 4. It is obvious that the flexural strength of the CS/HA scaffolds showed a sustained growth as intrinsic viscosity of CS increased. When $[\eta]_{CS} = 5.75 \times 10^{-4}$, the flexural strength reached 13.8 MPa, which was 2.5 times that of $[\eta]_{CS} = 0.26 \times 10^{-4}$ (5.5 MPa). This result reveals that high molecular weight can bring high strength for polymers. However, the porosity of the CS/HA scaffold showed an opposite trend, which decreased from 87.5 to 64.6% with the increase of $[\eta]_{CS}$ from 0.26×10^{-4} to 5.75×10^{-4}. In the preparation of CS/HA scaffold, solvent in the CS/HA system will freeze and expand during the process of freeze-drying. And the extent of expansion decreases as strength of CS molecular chain raises. So high intrinsic viscosity of CS will reduce porosity of CS/HA scaffold. It can be concluded that further increase of $[\eta]_{CS}$ will bring lower porosity to the CS/HA scaffold which cannot provide adequate bone repair capability. Besides, excessive high viscosity of CS will make it difficult to prepare the scaffold and HA powders cannot achieve a good dispersion in the CS solution. So when $[\eta]_{CS} = 5.75 \times 10^{-4}$, the CS/HA scaffolds prepared have both good mechanical property and suitable porosity.

Effect of Crosslinking Degree. Polysaccharides can be crosslinked by a reaction between the hydroxyl and amino groups of the chains with an appropriate agent to generate water insoluble crosslinked networks and to improve its mechanical strength and physicochemical properties.[27] In this article, glutaraldehyde (GA) was used as crosslinking agent to prepare GA-CS/HA scaffolds. GA is a homobifunctional crosslinker, which reacts with

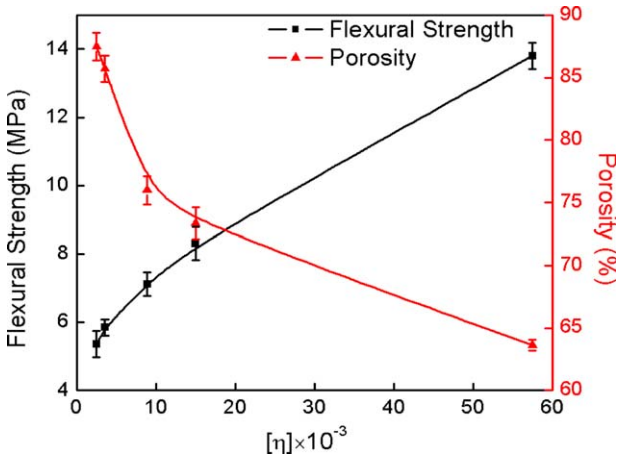

Figure 4. Effects of CS intrinsic viscosity on flexural strength and porosity of the CS/HA scaffolds. [Color figure can be viewed in the online issue, which is available at wileyonlinelibrary.com.]

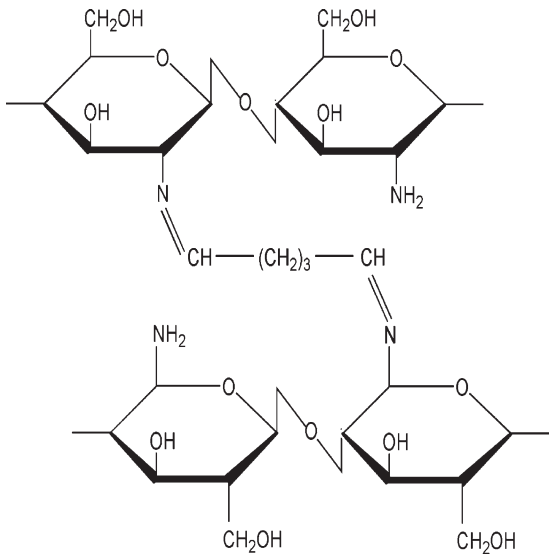

Scheme 1. The chemical structure of GA-crosslinked-CS.

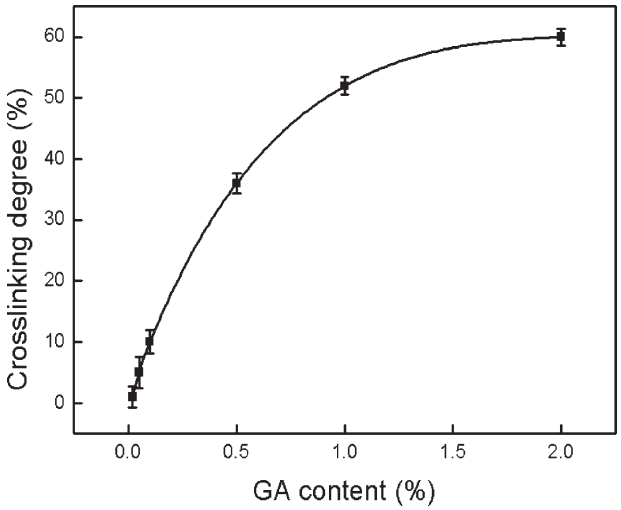

Figure 5. Relation of GA content and crosslinking degree of the CS/HA scaffolds.

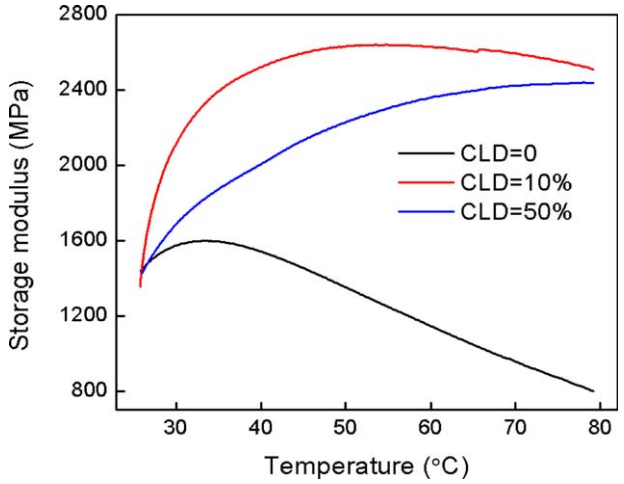

Figure 7. DMA of CS/HA samples with different crosslinking degree. [Color figure can be viewed in the online issue, which is available at wileyonlinelibrary.com.]

CS via either a Schiff base reaction, leading to imine functionality (Scheme 1, and/or through Michel-type adducts with terminal aldehydes, leading to the formation of carbonyl groups.[28]

The crosslinking degree (CLD) of the CS/HA scaffolds was measured by Soxhlet extractor (Figure 5. The CLD showed a markedly improvement from 0 to 52% with the GA content increased from 0 to 1%. However, the CLD increased slowly when the content of GA was >1%. Figure 6 provides the flexural strength and porosity of CS/HA scaffolds with different crosslinking degree. It can be seen that appropriate crosslinking is beneficial to improve the mechanical properties of CS/HA scaffolds. When GA content is small, low crosslinking degree may be favorable to a more regular arrangement between chitosan molecular chains. The formation of slight network structure maintains the crystal structure, thus increasing the mechanical strength.[29] When the CLD was 10%, the flexural strength of the CS/HA scaffold reached a maximum value of 20 MPa, which increased 45% compared with noncrosslinked scaffolds and has

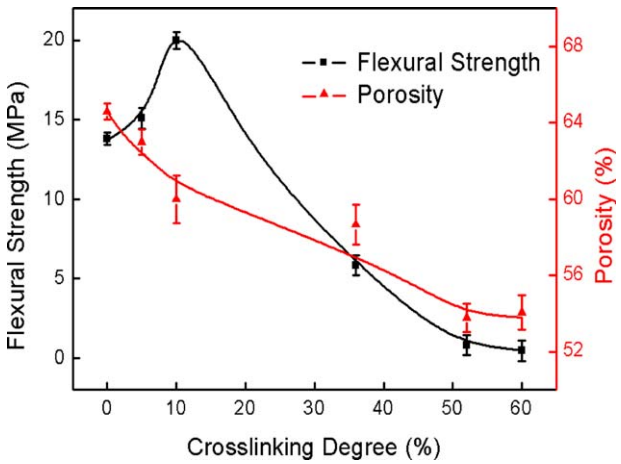

Figure 6. Effects of crosslinking degree on flexural strength and porosity of the CS/HA scaffolds. [Color figure can be viewed in the online issue, which is available at wileyonlinelibrary.com.]

met the demand of mechanical property of cancellous bone in human bone tissue.[30] However, if GA content increases further, higher crosslinking degree will bring excess crosslinking points and short molecular chain between each crosslinking points. As a result, the CS/HA scaffolds changes from a hard and tough material to a hard and brittle material. So the flexural strength of the CS/HA scaffold decreases rapidly. Moreover, when CLD = 10%, the scaffold had a porosity no <60%.

To investigate the effect of crosslinking degree on mechanical properties of CS, three samples with different crosslinking degree (CLD = 0, 10 and 50%, respectively) were prepared and their storage modulus was measured by DMA (Figure 7. Storage modulus (E) is proportion to the maximum elasticity which sample stores in each period. It can reflect the elastic component of viscous elastic materials and indicate material's ability to resist deformation.[31] The greater the modulus is, the less easily the samples deform, which means the greater rigidity the materials have. According to literature,[32] increase of crystallinity and crosslinking between molecules both can improve the rigidity of materials. Figure 7 indicates that the storage modulus of crosslinked CS is improved significantly in the test range. The noncrosslinked sample had a storage modulus of 1581 MPa under 37°C. When CLD = 10%, the storage modulus of the sample was 2452 MPa under the same temperature, which increased 54% compared with the noncrosslinked sample. However, storage modulus of the sample with 50% CLD under 37°C (1927 MPa) was lower than the sample with 10% CLD, which indicated that excessive crosslinking would, on the contrary, reduce the strength of sample. In brief, for a given temperature, the CS is significantly reinforced by appropriate crosslinking.

Characterization of CS/HA Scaffold

Morphology. The SEM images and apertures size distribution of the CS/HA scaffolds are provided in Figure 8. The SEM image shows that the scaffolds are porous. The pores are open, homogeneous and interconnected with an average diameter of 125 μm, which can provide appropriate three-demensional

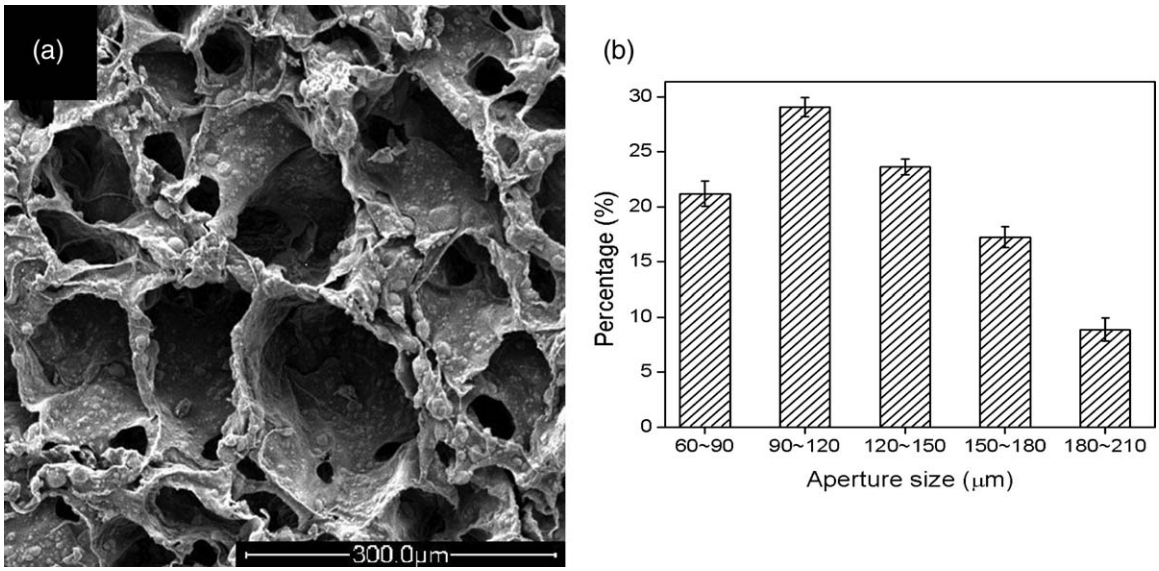

Figure 8. (a) SEM image of the CS/HA porous scaffold ($[\eta]$CS = 5.75 × 10^{-4}, HA content = 65%, CLD = 10%); (b) Apertures size distribution of the porous scaffold.

microstructure for growth of bone cells and nutrient circulation.[33] Meanwhile, the short rod-like HA particles disperse evenly in the CS/HA scaffold (Figure 9, which is similar with the human bone apatite particles.[34] The average length of HA is 113 nm. The homogeneous distribution of nano-HA particles on the scaffold surface can give more contacting areas for bone cells.

FTIR Analysis. Figure 10 shows the FTIR spectra of CS (a), HA (b), CS/HA scaffold (c), and GA-CS/HA scaffold (d). Curve a represents the IR bands of CS, including characteristic bands at 1644 and 1550 cm^{-1}, which correspond to the stretching of amide C═O (amide I) and N—H deformations of a primary amine (amide II).[35] Curve b is the IR spectrum of HA. The 3435 and 631 cm^{-1} peaks are assigned to the stretching and deformations of O═H. The bands at 1000–1100 and 568 cm^{-1} are attributed to v_3 and v_4 vibration of —PO_4 respectively.[36] For the CS/HA composite (curve c), the amide I peak shifts from 1644 to 1630 cm^{-1}. This red shift may be caused by the formation of hydrogen bond between ═OH of HA and ═NH_2 of CS and chelate effect between Ca^{2+} of HA and —NH_2 of CS. In curve d, the decrease of amide II peak at 1550 cm^{-1} is caused by the crosslinking reaction between GA and CS. In addition, an increase peak at 2900 cm^{-1} (which is the characteristic peak of C—H) indicates the introduction of glutaraldehyde.

XRD Analysis. The XRD spectra of CS/HA scaffolds with different HA content and crosslinking degree are provided in Figure

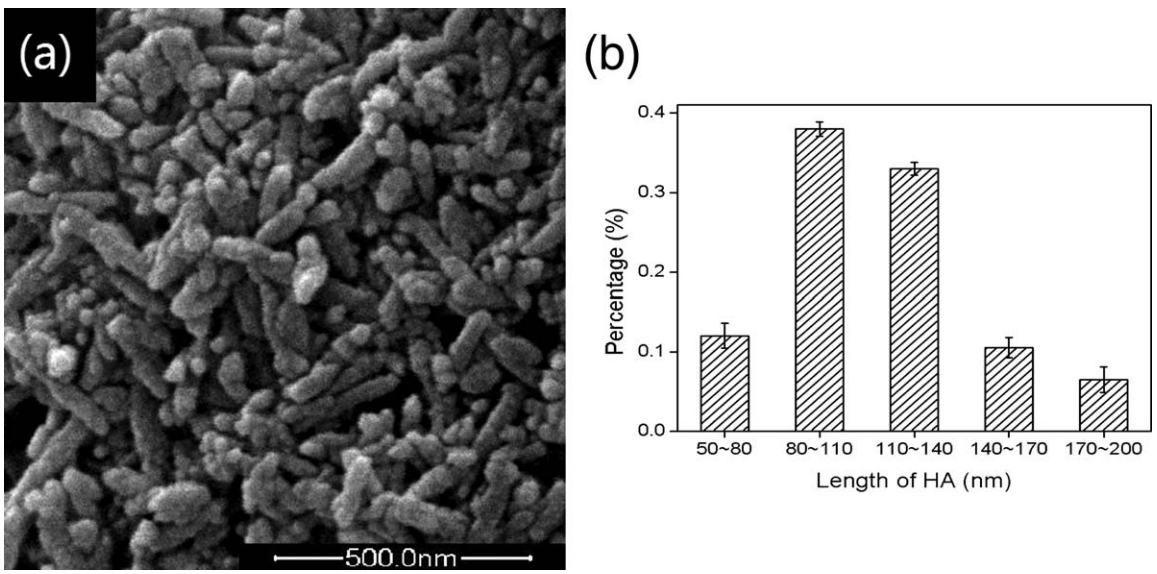

Figure 9. (a) SEM image of the HA particles in CS/HA scaffold ($[\eta]$CS = 5.75 × 10^{-4}, HA content = 65%, CLD = 10%); (b) Distribution of HA particles size.

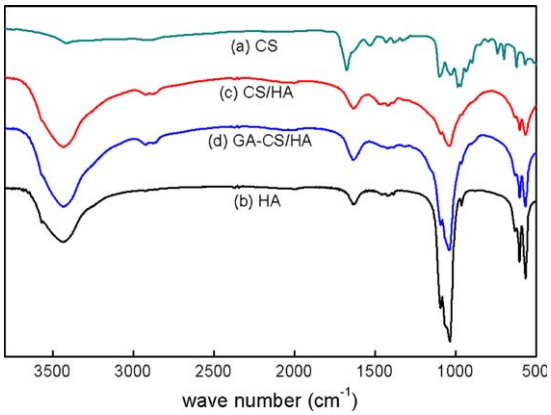

Figure 10. FTIR spectra of (a) CS; (b) HA; (c) CS/HA composites; (d) GA-CS/HA composites. [Color figure can be viewed in the online issue, which is available at wileyonlinelibrary.com.]

11. The characteristic 2θ peaks of HA powder are at ~25.8°, 32.9°, 34.0°, 39.9°, 46.7°, and 49.4° corresponding to the diffraction planes of (002), (300), (202), (130), (222), and (213) of the HA crystallites.[37] As a semicrystalline biopolymer, CS presents broad diffraction peaks at 19.8° and 21.9°. For the CS/HA composites, the typical crystalline peaks of both CS and HA still exist as shown in Figure 11. This indicates that the blending process did not cause significant change to the structure of CS and HA, which is very important for maintaining biological activity of CS/HA scaffold. When HA content increases from 10 to 65%, the characteristic peaks of CS become weaker significantly (curve a and b), which means the presence of HA will increase amorphous component of CS. The molecular interaction between CS and HA leads to hybridization and therefore affects the diffraction peaks. After crosslinked by GA, the diffraction peaks of CS almost disappear (curve c). The disappearance of CS 2θ peaks shows that the network structure was formed in CS/HA scaffold which decreased the crystallinity of CS.

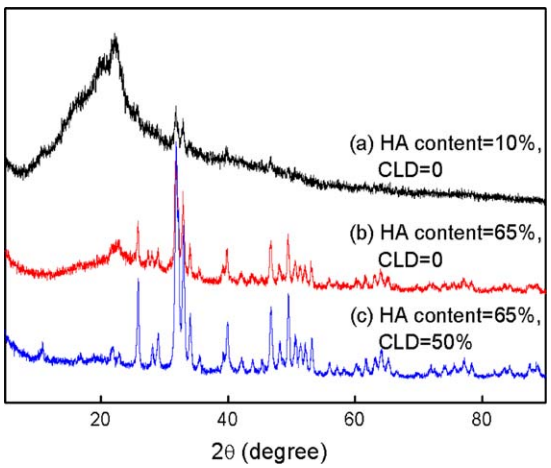

Figure 11. XRD spectra of (a) CS/HA composites with HA content = 10%; (b) CS/HA composites with HA content = 65%; (c) GA-CS/HA composites with HA content = 65%. [Color figure can be viewed in the online issue, which is available at wileyonlinelibrary.com.]

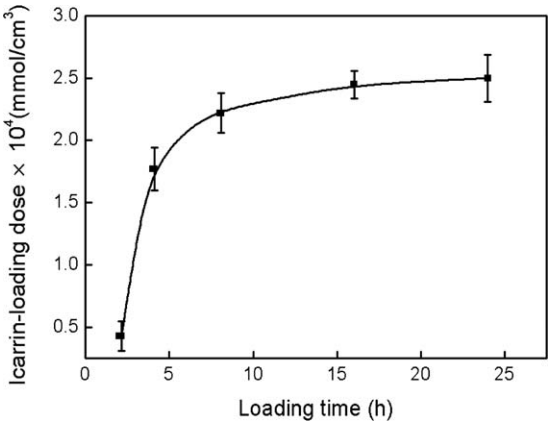

Figure 12. The influence of loading time on icariin-loading dose.

Study of Icariin-Loading-CS/HA Scaffold

Influence of Loading Time on Icariin Loading Dose. Five icariin-loading scaffolds were prepared with different loading time of 2, 4, 8, 16, and 24 h, respectively. It reveals that icariin-loading dose increased with the prolongation of loading time (Figure 12. When loading time was <2 h, the icariin dose was only 0.43×10^{-4} mmol cm^{-3}. Afterward, the icariin dose increased fivefold after 8 h, arriving at 2.22×10^{-4} mmol cm^{-3}. In the icariin solution, hydrogen bonds can easily form between hydroxyl groups in icariin molecules and amino groups in CS molecules. So icariin can be physical adsorbed in the scaffolds in a short period of time and a great increase of loading dose can be found. However, when the loading time was longer than 8 h, the icariin loading dose didn't change much, which reveals that the adsorption between icariin and scaffold tends saturation. Therefore, 24 h is enough for icariin to load on the CS/HA scaffold with the loading dose of 2.5×10^{-4} mmol cm^{-3}.

Influence of Crosslinking Degree on Icariin Loading Dose. The drug dose of icariin-loading-scaffolds with different crosslinking degree is shown in Figure 13. The icariin-loading dose of CS/HA scaffolds decreased gradually with the increase of crosslinking degree. When CLD = 10%, the icariin dose was 1.77×10^{-4} mmol cm^{-3}, and it dropped to 0.27×10^{-4} mmol cm^{-3} when CLD = 60%. The adsorption between

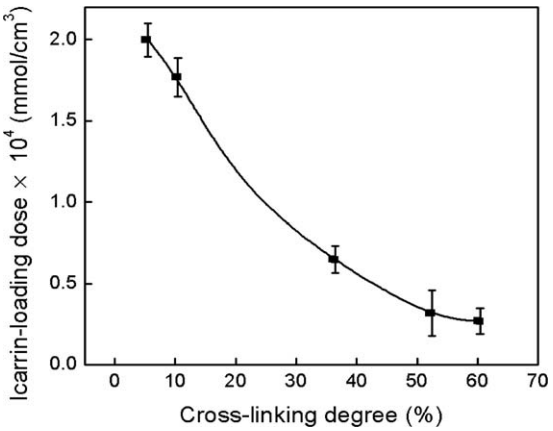

Figure 13. The influence of crosslinking degree on icariin-loading dose.

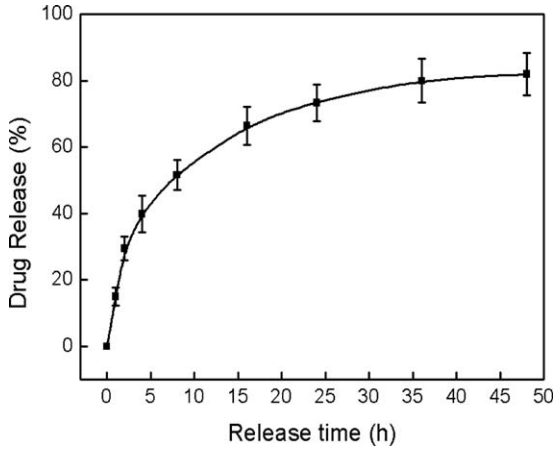

Figure 14. Release behavior of the icariin-loading CS/HA scaffolds.

scaffolds and icariin is mainly owing to the action of hydrogen bonds between CS and icariin molecules. However, the crosslink reaction between CS and GA will consume some hydroxyl groups and amino groups in CS molecule chains, thus the adsorption effect will be weakened. The higher crosslinking degree is, the lesser adsorption loading is. High crosslinking degree is not conducive to the adsorption of icariin for the CS/HA scaffold. Hence, it will be better to keep crosslinking degree no more than 10%.

Icariin Release Behavior. Ideal bone repair materials demand to release drug gradually in a long period of time which can promote the regeneration of bone tissue. The drug release curve of the icariin-loading-CS/HA scaffolds is shown in Figure 14. In the release pattern, about 50% of icariin was released rapidly in the first 8 h. Then the release slowed down gradually and drug release was 73% when release time reached 24 h. From 24 to 48 h, the release rate of icariin was very slow, and the equilibrious release was about 80%. Icariin is absorbed and stored in micro interspaces of the CS/HA scaffold. In the release medium, CS molecules expand with water immersion, then the icariin adsorbing on the surface or encapsulated in superficial layer of scaffold is released, and a quick release can be seen at the initial stage. As time go on, the swelling reaches equilibrium, and icariin adsorbing inside the scaffold can only be released by slow diffusion or scaffold degradation, thus icariin release rate is decreased. To sum up, taking the CS/HA scaffolds as drug carrier to load icariin can achieve basic drug sustained release effect and the release behavior obeys diffusion controlled mechanism.

CONCLUSIONS

The CS/HA bone repair scaffolds were successfully obtained through solution blending, crosslinking by GA and freeze-drying technique. The prepared CS/HA scaffolds were porous and average pore diameter was 125 μm, short rod-like HA particles dispersed evenly in the scaffolds with average length of 113 nm. When intrinsic viscosity of CS was 5.75×10^{-4} and HA content = 65%, the resulting CS/HA scaffold had both maximum flexural strength and high porosity. Appropriate crosslinking by GA could enhance the mechanical strength of the scaffolds. When CLD = 10%, flexural strength of the CS/HA scaffolds reached 20 MPa, which increased 45% compared with the noncrosslinked scaffolds.

The CS/HA scaffolds could be used as drug carrier to load icariin. About 24 h was enough for loading icariin on the scaffold. High crosslinking degree would weaken the hydrogen bonding effect between icariin and CS/HA scaffold, and then resulted in low-drug loading dose. The drug release test demonstrated that icariin could be sustained released from the icariin-loading CS/HA scaffolds.

ACKNOWLEDGEMENTS

The authors are grateful to the financial supports from the National Natural Science Foundation of China (81072958) and the Natural Science Foundation of Shanghai (11ZR1439300).

REFERENCES

1. Nakamatsu, J.; Torres, F. G.; Troncoso, O. P.; Lin, Y. M.; Boccaccini, A. R. *Biomacromolecules* **2006**, *7*, 3345.
2. Mohamed, K. R.; El-Rashidy, Z. M.; Salama, A. A. *Ceram. Int.* **2011**, *37*, 3265.
3. Chiono, V.; Gentile, P.; Boccafoschi, F.; Carmagnola, I.; Ninov, M.; Georgieva, V.; Georgiev, G.; Ciardelli, G. *Biomacromolecules* **2010**, *11*, 309.
4. Han, J.; Zhou, Z.; Yin, R.; Yang, D.; Nie, J. *Int. J. Biol. Macromol.* **2010**, *46*, 199.
5. Li, Z.; Kawashita, M. *J. Artif. Organs* **2011**, *14*, 163.
6. Kuo, S. M.; Chang, S. J.; Lin, L. C.; Chen, C. J. *J. Appl. Polym. Sci.* **2003**, *89*, 3897.
7. Alvarez, K.; Nakajima, H. *Materials* **2009**, *2*, 790.
8. An, J. S.; Nam, B. U.; Tan, S. H.; Hong, S. C. *Macromol. Symp.* **2007**, *249*, 276.
9. Wang, X.; Tan, Y.; Zhang, B.; Gu, Z.; Li, X. *J. Biomed. Mater. Res. A.* **2009**, *89*, 1079.
10. Modaress, M. P.; Mirzadeh, H.; Zandi, M. *Iran. Polym. J.* **2012**, *21*, 191.
11. Solchaga, L. A.; Temenoff, J. S.; Gao, J.; Mikos, A. G.; Caplan, A. I.; Goldberg, V. M. *Osteoarthr. Cartilage.* **2005**, *13*, 297.
12. Ye, L.; Zeng, X.; Li, H.; Wang, Z. *J. Appl. Polym. Sci.* **2009**, *116*, 762.
13. Ma, R.; Weng, L.; Bao, X.; Song, S.; Zhang, Y. *J. Appl. Polym. Sci.* **2013**, *127*, 2581.
14. Zuo, G.; Wan, Y.; Wang, L.; Liu, C.; He, F.; Luo, H. *Mater. Lett.* **2010**, *64*, 2126.
15. Céline, P. B.; Antoine, V.; Denis, B.; Laurent, V.; Laurent, D.; Catherine, F. *J. Appl. Polym. Sci.* **2013**, *128*, 2945.
16. Heinemann, C.; Heinemann, S.; Lode, A.; Bernhardt, A.; Worch, H.; Hanke, T. *Biomacromolecules* **2009**, *10*, 1305.
17. Muldaerjee, D. P.; Tunlde, A. S.; Roberts, R. A. *J. Biomed. Mater. Res. B.* **2006**, *67*, 603.
18. Zan, Q. F.; Wang, C.; Dong, L. M.; Tian, J. M. *Rare Metal Mater. Eng.* **2005**, *34*, 1204.

19. Chen, A. M.; Hou, C. L.; Tu, K. Y. *Acad. J. Sec. Mil. Med. Univ.* **1997**, *18*, 319.
20. Liu, B.; Zhang, H.; Xu, C.; Yang, G.; Tao, J.; Huang, J.; Wu, J.; Duan, X.; Cao, Y.; Dong, J. *Brain Res.* **2011**, *1375*, 59.
21. Zheng, D.; Peng, S.; Yang, S. H.; Shao, Z. W.; Yang, C.; Feng, Y.; Wu, W.; Zhen, W. X. *Bone* **2012**, *51*, 85.
22. Fan, J. J.; Cao, L. G.; Wu, T.; Wang, D. X.; Jin, D.; Jiang, S.; Zhang, Z. Y.; Bi, L.; Pei, G. X. *Molecules* **2011**, *16*, 10123.
23. Wu, T.; Nan, K.; Chen, J.; Jin, D.; Jiang, S.; Zhao, P.; Xu, J.; Du, H.; Zhang, X.; Li, J.; Pei, G. *Chin. Sci. Bull.* **2009**, *54*, 2953.
24. Xu, T.; He, D.; Zhou, Y. Y. *Opaedic Biomech. Meter. Clin. Study* **2008**, *5*, 44 (In Chinese).
25. Yang, Y.; Zhao, J.; Zhao, Y.; Wen, L.; Yuan, X.; Fan, Y. *J. Appl. Polym. Sci.* **2008**, *109*, 1232.
26. Sun, F.; Lim, B. K.; Ryu, S. C.; Lee, D.; Lee, J. *Mater. Sci. Eng. C Bio. S.* **2010**, *30*, 789.
27. Wang, J. J.; Zeng, Z. W.; Xiao, R. Z.; Xie, T.; Zhou, G. L.; Zhan, X. R.; Wang, S. L. *Int. J. Nanomed.* **2011**, *6*, 765.
28. Austero, M. S.; Donius, A. E.; Wegstand, U. G. K.; Schauer, C. L. *J. R. Soc. Interface* **2012**, *9*, 2551.
29. Chen, X.; Shao, Z. Z.; Huang, Y. F.; Huang, Y.; Zhou, P.; Yu, T. Y. *Acta Chim. Sin.* **2000**, *58*, 1654.
30. Xu, X. Y.; Liu, T. T.; Zheng, J.; Li, Y. *Mater. Rev.* **2012**, *26*, 102 (In Chinese).
31. Webb, A. R.; Yang, J.; Ameer, G. A. *J. Polym. Sci. Polym. Chem.* **2008**, *46*, 1318.
32. Yeong, T. S.; Hui, C. C. *J. Appl. Polym. Sci.* **2001**, *81*, 1808.
33. Budiraharjo, R.; Neoh, K. G.; Kang, E. T. *J. Colloid Interf. Sci.* **2012**, *366*, 224.
34. Klinkaewnarong, J.; Swatsitang, E.; Maensiri, S. *Solid State Sci.* **2009**, *11*, 1023.
35. Li, J.; Zhu, D.; Yin, J.; Liu, Y.; Yao, F.; Yao, K. *Mater. Sci. Eng. C Bio. S.* **2010**, *30*, 795.
36. Liu, C.; Ji, X.; Cheng, G. *Appl. Surf. Sci.* **2007**, *253*, 6840.
37. Sreedhar, B.; Aparna, Y.; Sairam, M.; Hebalkar, N. *J. Appl. Polym. Sci.* **2007**, *105*, 928.